P5.13 Cloud Detection from MISR using a Band-Differenced Angular Signature

Michael Wilson and Larry Di Girolamo
University of Illinois at Urbana-Champaign
Urbana, IL

1. Introduction

Cloud detection has historically been prone to more uncertainty in the polar regions than other regions of the earth. Low-level clouds and snow have similar radiation properties in visible and near-infrared channels, especially in nadir views. Since satellites have historically used nadir views for cloud detection, large errors in cloud detection for snow and ice covered regions have been typical. However, through the use of the Multi-angle Imaging SpectroRadiometer (MISR) on-board EOS Terra, coincident nadir and non-nadir visible/near-IR radiation measurements are now a possibility, which has the potential to circumvent the errors that have plagued previous satellite measurements.

MISR provides multi-angle coverage of the earth at nine specific angles: 0°, ±26.1°, ±45.6°, ±60°, and ±70.5°. This is done using 9 separate cameras, four of which view in the forward direction with respect to the satellite orbital track, one which views at nadir, and four which view in the aft direction. Each camera has four spectral channels: the blue band, the green band, the red band, and the near-infrared band (443 nm, 555 nm, 670 nm, and 865 nm respectively). MISR operates in a push broom fashion, with a cross-track resolution of 275 m, and a swath width of approximately 360 km (For more information on the specifications of MISR, see Diner et. al., 1998).

The ability of MISR to make multi-angle measurements of the same scene creates new opportunities for cloud detection in the polar regions. While clouds, snow and ice may all appear to be approximately the same in nadir views, in non-nadir views, the radiative scattering properties have a much larger contrast. This led Di Girolamo and Davies (1994) to develop the Band-Differenced Angular Signature (BDAS), which will be shown to be effective at cloud detection for the polar regions.

The BDAS technique utilizes both the capability of MISR to measure at multiple angles and the capability of MISR to measure at multiple wavelengths. The BDAS takes the difference between the 443 nm and the 865 nm for two cameras: the camera at 60 degrees measuring forward scattered radiation, and the camera at 70.5 degrees measuring forward scattered radiation. Once the wavelengths have been differenced, the 70.5 degree band-differenced result is subtracted from the 60 degree band-differenced result, to create the BDAS.

Corresponding Author Address: Michael Wilson
105 S. Gregory St., Urbana, IL 61801
email: Wilson@atmos.uiuc.edu

The BDAS works due to differences in the forward-scattering properties of clouds and surface features. For example, figure 1 shows that clouds and surface features are very similar for the differenced wavelength between the blue and near-ir channels, except in the forward-scattered direction. In addition, the BDAS is sensitive to molecular scattering contributions above cloud tops. Longer path lengths through the molecular atmosphere tend to lead to higher levels of scattered blue light reaching the MISR sensor. Higher clouds shorten the path length that solar radiation takes through the atmosphere, and thereby reduces the amount of atmospherically-scattered blue light that reaches each MISR camera, compared to longer wavelengths. As a result, the BDAS is sensitive to higher clouds. Figure 1 shows that the differenced-wavelength value tends to increase towards the more oblique angles in the forward-scattered direction for clear conditions, while it decreases for cloudy regions. Therefore, the contrast between clouds and surface features can be measured by taking the slope of the lines between the most oblique cameras (i.e. differencing the two most oblique cameras). The results of Figure 1 are qualitatively consistent with the theoretical results of Di Girolamo and Davies (1994).

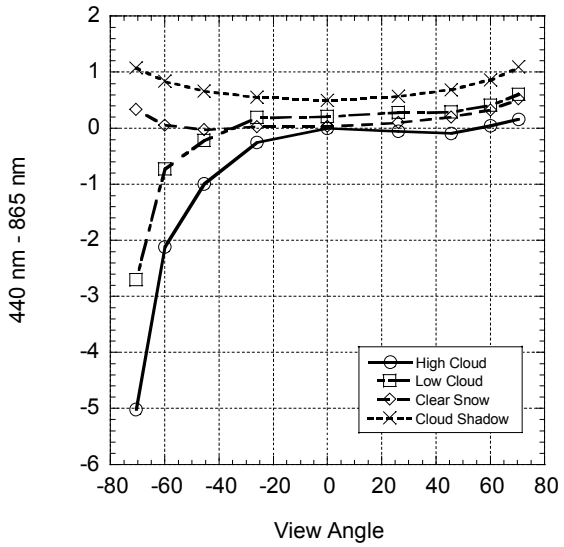

Figure 1: Demonstration of Difference between Blue and IR bands with respect to scattering angle. Negative values of view angle represent the forward-scattered direction. Positive values of view angle represent the back-scattered direction. This example was taken from MISR orbit 6865 over Antarctica. The symbols are positioned at the 9 MISR view angles.

2. Method

Seven scenes over the Greenland land mass were chosen for this particular study (see table 1).

Greenland was chosen because of the presence of a constant ice sheet over the region, especially during the summer. Since MISR can only operate in daylight conditions, scenes were chosen during the summer, so that enough daylight would be present for analysis.

Orbit #	Block #	Date	Average SZA
2713	28	Jun 21, 2000	53.405
3006	22	Jul 11, 2000	61.895
3455	37	Aug 11, 2000	51.165
3458	20	Aug 11, 2000	71.175
3459	17	Aug 11, 2000	74.760
3470	29	Aug 12, 2000	60.830
3475	12	Aug 12, 2000	81.070

Table 1: Orbit number, block number, observation date, and average solar zenith angle for the block of the MISR data used in this study.

Four consecutive blocks were chosen for each scene, based upon the availability of valid data, limited oceanic presence, and existence of surface and cloud features in each scene. Each block covers approximately 360 km cross-track, and 128 km along-track. Since MISR has multiple camera angles, it has the unique ability to determine stereo heights of objects in any scene. This effect can be visually achieved by placing all nine terrain-projected images of a scene into an animated sequence. In this sequence, surface features remain still for all nine images, while higher level features (such as clouds) move between scenes. This novelty of MISR allowed for the creation of a truth set, which greatly aided in determining appropriate thresholds for the BDAS and individual cameras in this study.

Once the animated scenes were developed, one block from each group of four was chosen for thresholding purposes. Multiple blocks could have been taken from each scene for thresholding, but by choosing only one block from each scene, any dependence based on scene choice was minimized. The BDAS was compared to the near-IR reflectance of the nadir and the most oblique camera in the forward-scattered direction for cloud detection. Thresholds were set manually for each individual scene.

This method did not take into account changes in the solar zenith angle between scenes. Within each scene, the solar zenith angle did not vary by more than three degrees. However, between all seven scenes, the solar zenith angle varies by over thirty degrees. Such a drastic change in solar zenith angle does have an effect on the chosen threshold for a given scene, as is illustrated by figure 2. In this figure, each case is placed in order according to the chosen BDAS threshold. A trend appears to be present between increased solar zenith angle and increased choice for a threshold.

The quality of each threshold was also checked to determine whether cloudy and clear pixels could adequately be separated by any given threshold. This factor became critical in the nadir near-IR thresholding cases, where as many as four of the seven cases had major misclassification errors that could not be reduced with any applied threshold.

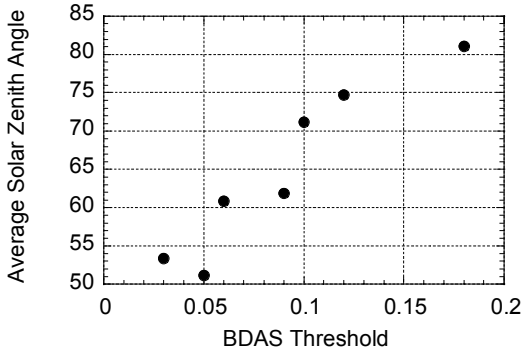

Figure 2: Solar Zenith Angle vs. BDAS Threshold. Note that as the chosen BDAS threshold increases, the average solar zenith angle also tends to increase.

3. Results

The BDAS technique and the near-IR thresholding for the most oblique camera (hereafter referred to as the oblique thresholding technique) appear to be statistically similar. Figure 3 shows the cloud fractions for each scene, using a manually determined threshold. All of the methods seem to show the general amount of cloud cover, but the oblique threshold technique and the BDAS technique tend to be similar, while the nadir values are more different. In addition, the manual thresholds applied to the nadir cameras were poor for over half of the cases, due to very bright surface features and dim clouds. Therefore, the BDAS and the oblique thresholding method appear to be much better suited to polar cloud detection than the traditional nadir thresholding method.

The graphs seem to indicate that the BDAS and the oblique thresholding method are very similar. However, the scenes have more differences than the graphs indicate. For example, in the case of orbit 3455, block 37 (see figure 4a), the oblique thresholding method can not detect clouds on the left side of the image, without misclassifying some clear region as cloud on the right side of the image (figure 4b). This occurs because the clouds on the left side of the image have a lower oblique camera near-IR value than the clear regions on the right side of the image. The BDAS threshold can create a proper threshold for both sides of the image, but some regions in the interior of large clouds get misclassified as clear (figure 4c). While the cloud fraction difference is just above 6% between the two types, the quality of those thresholds is quite different. The nadir near-IR thresholding techniques are very different from both the oblique near-IR thresholds and the BDAS thresholds (figure 4d). The contrasts between clouds, snow, and ice are minimized in the nadir images, which leads to the largest chance of cloud misclassification. The quality of the nadir thresholds is much lower than for either the BDAS thresholds or the oblique near-IR thresholds. Figure 4 represents the worst performance of the seven scenes examined.

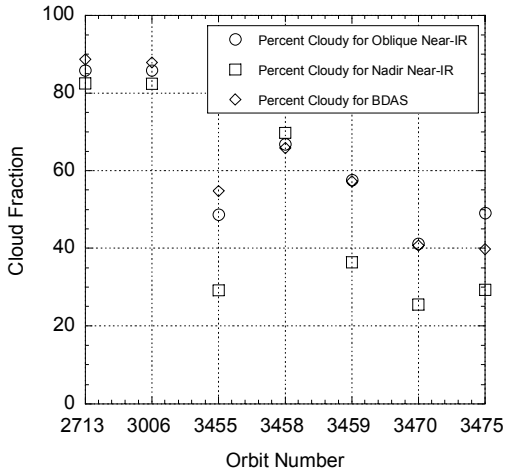

Figure 3: The percentage of each scene that was classified as cloudy by each manually determined threshold.

4. Conclusion

Cloud detection through visible and near-infrared channels has been error-prone in the polar regions due to the similar radiative properties of snow and ice in the nadir viewing directions. Through the use of MISR, however, polar cloud detection can be improved. Oblique cameras in the forward-scattering directions tend to measure stronger contrasts between surface and cloud features than do nadir measurements.

Nadir images tended to have more cloud misclassification for any manually applied threshold, compared to the oblique thresholds and BDAS thresholds. Since the thresholds do depend on solar zenith angle, future studies should explore the relationship between chosen threshold and average solar zenith angle. A threshold range dependent on solar zenith angle may give a more accurate representation of the true cloud cover in the arctic and antarctic.

The cloud fractions seem to indicate that oblique near-IR thresholding methods and BDAS thresholding methods are approximately equal in their ability to determine cloud cover. However, the near-IR method tends to miss some clouds, while the BDAS method tends to miss small parts of clouds. The result is a small difference between cloud fractions, but for different reasons. The nadir thresholds were of significantly worse quality on average, even when cloud fractions were similar, because much more misclassification occurred using the nadir method than for either the oblique or BDAS method. Cameras at non-nadir angles have much more potential than nadir cameras for cloud detection in polar regions, due to the different scattering properties of clouds and surface features in the forward scattering direction. This study shows that non-nadir measurements are more reliable than nadir measurements. In addition, the BDAS method has the ability to detect more clouds than near-IR thresholding on the oblique cameras. However, seven scenes are not enough to draw strong statistical conclusions. Therefore, more study must be done in order to create an automatic thresholding method for the polar regions.

References:

Diner, D. J. and co-authors, 1998: Multi-angle Imagine SpectroRadiometer (MISR) description and experiment overview. *IEEE Trans. Geosci. Remote Sens.* 36, 1072-1087.

Di Girolamo, L. and R. Davies, 1994: A Band-Differenced Angular Signature Technique for Cirrus Cloud Detection. *IEEE Trans. Geosci. Remote Sens.* 32, 890-896.

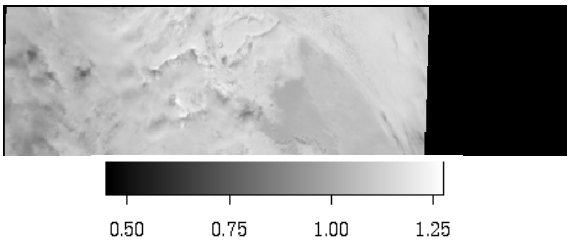

Figure 4a: Orbit 3455, Block 37, oblique near-IR image.

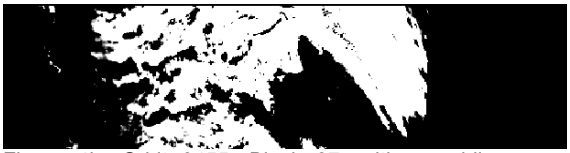

Figure 4b: Orbit 3455, Block 37, with an oblique near-IR threshold of 1.0. All white regions are cloudy, all black regions are clear.

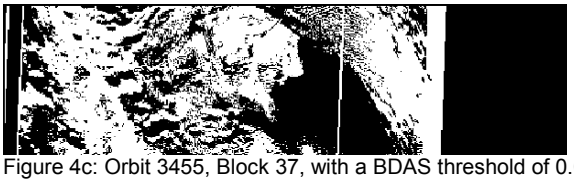

Figure 4c: Orbit 3455, Block 37, with a BDAS threshold of 0.05. All white regions are cloudy, all black regions are clear. Semi-vertical stripes are no retrieval. Note that the striped regions were not used in the calculation of the BDAS cloud fractions.

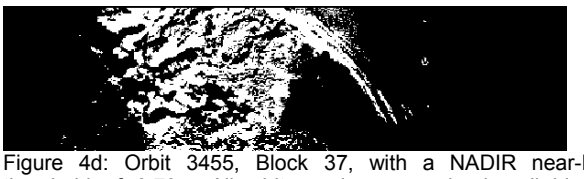

Figure 4d: Orbit 3455, Block 37, with a NADIR near-IR threshold of 0.79. All white regions are cloudy, all black regions are clear.